Catalytic isomerization of 1-hexene to 2-hexene by halide clusters of Nb, Mo, Ta and W possessing an octahedral metal core

Satoshi Kamiguchi [a], Miaki Noda [b], Yuka Miyagishi [b], Satoru Nishida [b], Mitsuo Kodomari [b], Teiji Chihara [a],*

[a] *The Institute of Physical and Chemical Research (RIKEN), Wako, Saitama 351-0198, Japan*
[b] *Shibaura Institute of Technology, Faculty of Technology, Shibaura, Minato-ku, Tokyo 108-8548, Japan*

Abstract

Halide clusters, $[(M_6Cl_{12})Cl_2(H_2O)_4] \cdot 4H_2O$ (M: Nb, Ta) and $(H_3O)_2[(M_6Cl_8)Cl_6] \cdot 6H_2O$ (M: Mo, W) with an octahedral metal framework, develop catalytic activity for the isomerization and slight hydrogenation of olefinic double bonds when the halide clusters are treated in a stream of hydrogen at elevated temperatures. In the case of Nb clusters, treatment above 200 °C produces the catalytic activity. Raman spectra of such heat-treated clusters show that the cage breathing motion of Nb_6 remains intact, whereas the breathing vibrations of the edge bridging Nb–Cl of $[Nb_6Cl_{12}]$ disappear. In the case of W clusters, the catalytic activity appears at 300 °C, at which temperature the structure of $[(W_6Cl_8)Cl_4(H_2O)_2]$ begins to decay to form W_6Cl_{12}. Maximum activity emerges at 450 °C, at which temperature the structure of W_6Cl_{12} begins to decay. Elemental analyses of both clusters show the loss of Cl atoms. Thus, activation of these clusters occurs by partial loss of the halogen ligands, leaving the cluster framework intact.
© 2002 Elsevier Science B.V. All rights reserved.

Keywords: Isomerization of olefin; Catalysis by halide cluster; Retention of cluster framework; Niobium halide; Tungsten chloride

1. Introduction

Extensive effort has been made towards the syntheses of new halide clusters or combining known halide clusters with new networks [1–3]. The application of these clusters has focused mainly on their electronic and magnetic properties. Studies on the reactivity of cluster halides have been quite limited. Reactivity with organic or inorganic reagents can be seen predominantly in the field of ligand exchange reactions, and occasionally the reaction of hydrogen

[4,5] with a halide cluster has been reported. Aside from our preliminary report [6], we are unaware of any report of the use of halide clusters as catalysts [7–9]. Carbonyl clusters, on the other hand, are heavily associated with catalysis, with most of these clusters containing platinum group metals. These metals have versatile catalytic activities in both homogeneous and heterogeneous systems. However, carbonyl clusters are thermally unstable. Almost all decompose above 200 °C due to their inherently weak metal–metal bonds. Hence, reactions catalyzed by clusters with intact metal frameworks are rare [10]. Isolation and characterization of molecular clusters is relatively simple. Thus, they provide good models of metal catalysts. Halide clusters are generally

---

* Corresponding author. Tel.: +81-48-467-9399;
fax: +81-48-462-4631.
E-mail address: chihara@postman.riken.go.jp (T. Chihara).

synthesized by comproportionation of a metal with the corresponding mononuclear metal halide at elevated temperatures (generally 600–1000 °C) for several days to weeks in a sealed tube, implying that halide clusters are too stable to react with organic substances. Evidently, the thermal stability of halide clusters prevents attempts to utilize them as catalysts. Since metal–metal bonds of the group V and VI 4d and 5d metals are stronger than their platinum group counterparts, an uncoordinated metal center could be revealed leaving the thermally stable metal framework intact, if some of the ligands are removed. Most halide clusters have octahedral metal array structures consisting of the pure metal crystals, with terminally coordinating, bridging, or triply bridging halogen π-donor ligands. The oxidation number of the metal atoms in the cluster is approximately +2, which is the average of those of the oxide and neutral bulk metal. The catalytic activity, as well as the reactivity of the metal atom in the middle oxidation states, has not been reported. Moreover, the concerted effect of the metal–metal bonds of the cluster is also unknown. Hydrogen was chosen as an activation reagent for the cluster, as hydrogen is a simple gaseous molecule and can yield hydrogen chloride while leaving a hydride ligand in the cluster. Either one hydride ligand with two coordinatively unsaturated sites or three of these is enough for hydrogenation and isomerization of an olefin in the case of a mononuclear complex [11]. Three coordinatively unsaturated sites or equivalent active sites for M_6 of the cluster are enough for the reaction, assuming that the remaining halogen ligands are fluxional. This would correspond to only a half-active site for each metal atom. Moreover, more extensive activation would give rise to various types of reactions with retention of the cluster framework. Thus, a simple reaction of olefin with hydrogen was chosen as a test reaction for the cluster catalysis, and successful catalysis of isomerization is reported here.

Platinum group metals and Ni are used practically for the isomerization and hydrogenation of olefins in heterogeneous systems [12–15]. No metal halides, except $TiCl_3$ [16], have been reported as isomerization catalysts of olefins in heterogeneous systems, although metal sulfides and oxides of group V and VI metal compounds have been reported to catalyze the reaction.

2. Experimental

2.1. Materials and characterization

The cluster complexes $[(Nb_6Cl_{12})Cl_2(H_2O)_4] \cdot 4H_2O$ (**1**) [17], $[(Nb_6Br_{12})Br_2(H_2O)_4] \cdot 4H_2O$ [17], $(H_3O)_2$ $[(Mo_6Cl_8)Cl_6] \cdot 6H_2O$ [18], $[(Ta_6Cl_{12})Cl_2(H_2O)_4] \cdot$ $4H_2O$ [17], and $(H_3O)_2[(W_6Cl_8)Cl_6] \cdot 6H_2O$ (**2**) [19] were prepared according to published procedures. The solid state cluster W_6Cl_{12} $([W_6Cl_8^i]Cl_2^aCl_{4/2}^{a-a}$ (**3**) was obtained by heating **2** at 67 °C/h to 450 °C and holding at 450 °C for 1 h [20]. The complex Re_3Cl_9 $([Re_3Cl_3^i]Cl_3^aCl_{6/2}^{a-a})$ was commercially available (Furuya Metal) and used without further purification. The crystals of the complexes were crushed and screened to 150−200 mesh. 1-Hexene (>99%, Aldrich) was used as received. Hydrogen (99.999%) was generated by hydrolysis of water (Whatman). Powder X-ray diffraction (XRD) was performed with a Rigaku RAD-3R X-ray diffractometer using Cu Kα radiation at a scan rate of 2°/min. Raman spectra were recorded on a Kaiser Optical Systems HoloLab 5000 with an Nd:YAG laser operating at 532 nm with a 7.6 mm focus lens. Counts were accumulated 30 times at 1 s intervals. Elemental analysis was performed by the Chemical Analysis Section of this institute (RIKEN). The products were analyzed by GC/MS (Hewlett-Packard 5890 Series II gas chromatograph coupled with a Jeol Automass System II, a 15 m × 0.25 mm × 0.25 μm DB-1 capillary column, helium carrier gas) and GLC (GL Sciences 353B gas chromatograph fitted with a flame ionization detector, a 30 m × 0.25 mm × 0.25 μm DB-1 capillary column, helium carrier gas). All of the products were identified by comparison with authentic samples obtained commercially. The catalytic activities were analyzed by an on-line GLC. (Shimadzu 7A gas chromatograph fitted with a flame ionization detector, a 10 m × 3 mm 25% sebaconitrile on Uniport C packed column, nitrogen carrier gas.)

2.2. Catalytic measurement

The reaction apparatus used for the preliminary treatment of the cluster and subsequent catalytic reaction is shown in Fig. 1. A weighed cluster sample (30 mg) was placed in a Pyrex (up to 500 °C) or quartz (550−600 °C) tube (3 mm i.d.) surrounded closely
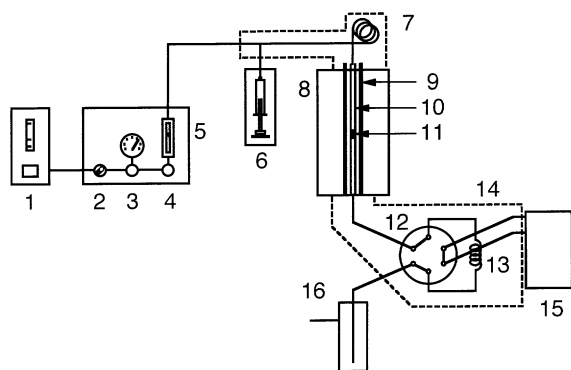
Fig. 1. Schematic drawing of the reaction system: 1, hydrogen generator; 2, stop valve; 3, pressure regulator; 4, mass flow controller; 5, flow meter; 6, microfeeder; 7, preliminary heater for reaction gas; 8, oven; 9, copper jacket; 10, glass reactor; 11, catalyst; 12, six-way valve; 13, sampler loop; 14, heater for gas sampler; 15, on-line GLC; 16, trap bottle.

with a copper tube, and placed in the center of an electric furnace. The catalyst sample was given a preliminary treatment between room temperature and 600 °C for 1 h in a stream of hydrogen (40 ml/min). The reaction was initiated by feeding 1-hexene (10 mg/min) into the stream of hydrogen using a microfeeder at the same temperature, or constant temperature of 150 or 250 °C. The reaction was monitored by sampling the reaction gas (1 ml) with a six-way valve every 15 min followed by analysis using the on-line GLC. Analy-

ses of both liquid and gas products revealed that the main products are hexane and *cis*- and *trans*-2-hexene with a trace amount of *cis*- and *trans*-3-hexene. The total amount of 3-hexene was no more than 1% at 30% conversion and was thus ignored. No products other than those resulting from isomerization and hydrogenation were detected. The conversion was proportional to the amount of catalyst used, insofar as the conversion did not exceed 30%. Raman spectra of the sample in the stream of hydrogen were measured without removing the sample from the tube.

3. Results and discussion

3.1. Catalysis by halide clusters

Pulverized crystals of $[(Nb_6Cl_{12})Cl_2(H_2O)_4]\cdot 4H_2O$ (**1**) were packed into a glass reaction tube and heated in a stream of hydrogen for 1 h. Reaction was initiated by introduction of 1-hexene into the stream of hydrogen. A typical reaction profile is plotted in Fig. 2. Cluster **1** catalyzed isomerization and slightly catalyzed hydrogenation of the olefinic bond to yield *cis*- and *trans*-2-hexene and hexane. No other reactions were observed. Although the catalytic activity decreased with time, the *cis*/*trans* selectivity of the isomerized product 2-hexene remained constant. Table 1 lists the catalytic activity of various halide clusters and related
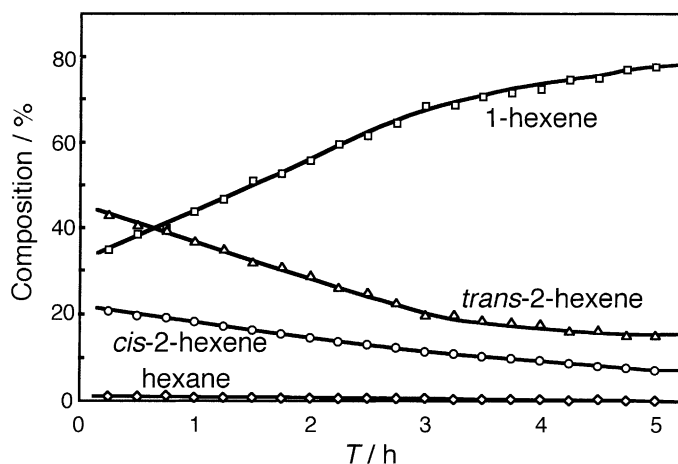

Fig. 2. Typical reaction profile of 1-hexene with hydrogen over $[(Nb_6Cl_{12})Cl_2(H_2O)_4]\cdot 4H_2O$ (**1**). Following treatment of **1** (30 mg) in a stream of H_2 (40 ml/min) at 350 °C for 1 h, reaction was started by the introduction of 1-hexene (10 mg/min) to the H_2 stream at the same temperature.

Table 1
Activity of halide cluster catalysts[a]

Catalyst	Conversion (%)	
	Isomerization[b] (*cis/trans*)	Hydrogenation[c]
$[(Nb_6Cl_{12})Cl_2(H_2O)_4] \cdot 4H_2O$ (**1**)	31.3 (0.47)	0.3
1[d]	25.5 (0.60)	0.0
$[(Nb_6Br_{12})Br_2(H_2O)_4] \cdot 4H_2O$	0.75 (0.47)	0.0
$[(Nb_6Br_{12})Br_2(H_2O)_4] \cdot 4H_2O$[e]	35.9 (0.45)	0.4
$(H_3O)_2[(Mo_6Cl_8)Cl_6] \cdot 6H_2O$	1.8 (0.78)	0.1
$[(Ta_6Cl_{12})Cl_2(H_2O)_4] \cdot 4H_2O$	1.4 (0.45)	0.1
$(H_3O)_2[(W_6Cl_8)Cl_6] \cdot 6H_2O$ (**2**)	1.8 (0.62)	0.1
Re_3Cl_9	0.0 (–)	0.0
Pt metal[f]	2.3 (0.75)	4.8
Pd metal[f]	5.4 (0.56)	1.1
Nb metal	0.0 (–)	0.0
No catalyst	0.0 (–)	0.0

[a] Catalyst was treated at 250 °C for 1 h followed by reaction at the same temperature, and the data were recorded after 4 h of reaction. Catalyst: 30 mg (150−200 mesh), H_2: 40 ml/min, 1-hexene: 10 mg/min.

[b] Isomerization = 2-hexene/(1-hexene + 2-hexene + hexane) × 100 (%) at 4 h.

[c] Hydrogenation = hexane/(1-hexene + 2-hexene + hexane) × 100 (%) at 4 h.

[d] He (40 ml/min) was used instead of H_2.

[e] Catalyst treatment and reaction was performed at 350 °C.

[f] Unsupported metal black powder. Catalyst powder was diluted with quartz sand (30 mg) before being charged into the reactor.

compounds treated in the same way. This table shows that Nb metal had no catalytic activity under the same reaction conditions. Niobium pentachloride cannot be applied to the catalysis under the same reaction conditions, as its boiling point is as low as 250 °C. These results clearly show that the halide cluster of Nb developed into a novel catalyst. Table 1 shows also that the cluster bromide of Nb and chlorides of Mo, Ta and W with octahedrally arranged M_6 metal cores showed catalytic activity for the isomerization of olefins. Although rhenium metal [21] and rhenium sulfides [22] have been reported to be hydrogenation catalysts, a rhenium cluster, Re_3Cl_9, with a triangular metal core had no catalytic activity under the same reaction conditions. The catalytic activity varied with the catalyst employed; however, the *cis/trans* selectivities of 2-hexene remained in a relatively narrow range and the ratios are approximately in accord with that of thermal equilibrium (0.77 at 250 °C) [23,24]. Isomerization of 1-butene to *cis*- and *trans*-2-butenes has been extensively studied over many heterogeneous basic and acidic catalysts. High *cis/trans* ratios have been observed over basic catalysts [25] such as MgO (3.2–7.0) [26], ZrO_2 (7.3) [27], and ThO_2 (3.1–3.4) [28], and low ratios over acidic catalysts such as $Nb_2O_5 \cdot nH_2O$

(2) [29], WO_2 (1.4) [30], and WO_3 (1.4) [30]. The corresponding *cis/trans* ratio of 2-hexene has not been reported on basic catalysts; however, on acidic catalysts the values reported are low: 0.83 on HY zeolite [31] and 0.5 on H-ZSM-5 [32]. Thus, the halide clusters might be classified as acidic catalysts. Table 1 also shows that the halide clusters are clearly distinguished from the platinum group metals by the low hydrogenation activities. The catalytic activities of the cluster catalysts listed in Table 1 are low compared with those of Pt and Pd. However, such a comparison is moot, since these two are in the form of amorphous black powder and the clusters used here are pulverized crystals. Our preliminary experiments showed that the catalytic activity is enhanced more than 100 times when the clusters are supported on silica gel.

3.2. Catalysis by $[(Nb_6Cl_{12})Cl_2(H_2O)_4] \cdot 4H_2O$ (**1**)

Reaction profiles of 1-hexene catalyzed by **1** at different temperatures are shown in Fig. 3. No catalytic activity was observed below 100 °C, indicating that the intact cluster is devoid of activity. Catalytic activity developed slightly when the reaction was performed
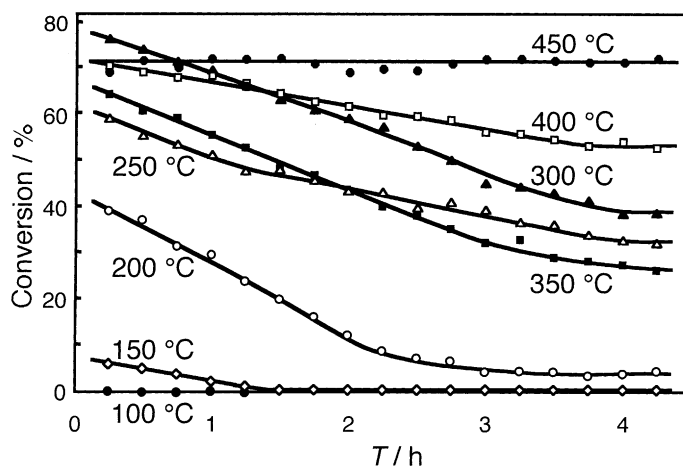
Fig. 3. Reaction profile of 1-hexene catalyzed by $[(Nb_6Cl_{12})Cl_2(H_2O)_4] \cdot 4H_2O$ (**1**) at different temperatures. After treatment of **1** (30 mg) with H_2 (40 ml/min) for 1 h, reaction was started by introduction of 1-hexene (10 mg/min) to the H_2 stream at the same temperatures. Conversion = (2-hexene + hexane)/(1-hexene + 2-hexene + hexane) × 100 (%).

at 150 °C, but soon waned. Heating above 250 °C gave the Nb cluster substantial catalytic activity, which was further enhanced with increasing temperature. The effect of the preliminary-treatment temperature of **1** on the catalytic activity was examined. The cluster samples were given a preliminary treatment by changing the temperature for 1 h, followed by reaction with 1-hexene at 150 °C. The catalytic activities decreased

with time, but converged to constant activities after 3 h. As Fig. 4 shows, preliminary treatment at around 200 °C gave the maximum activity to **1**; although apparent activity increased with increasing temperature, having a maximum activity at 300 °C, when both the preliminary-treatment and reaction temperatures were changed concurrently. The Raman spectra of **1** treated at various temperatures in hydrogen streams for 1 h
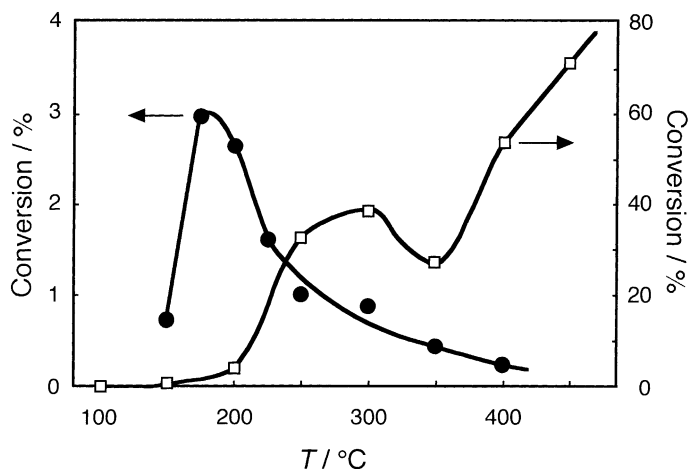

Fig. 4. Effect of treatment temperature on catalytic activity of $[(Nb_6Cl_{12})Cl_2(H_2O)_4] \cdot 4H_2O$ (**1**). After treatment of **1** at various temperatures for 1 h with H_2, reactions proceeded at the same temperature (□). After treatment of **1** at various temperatures for 1 h, reactions proceeded at 150 °C (●). Other conditions are the same as in Fig. 3. Conversion = (2-hexene + hexane)/(1-hexene + 2-hexene + hexane) × 100 (%) at 4 h after the reaction started.
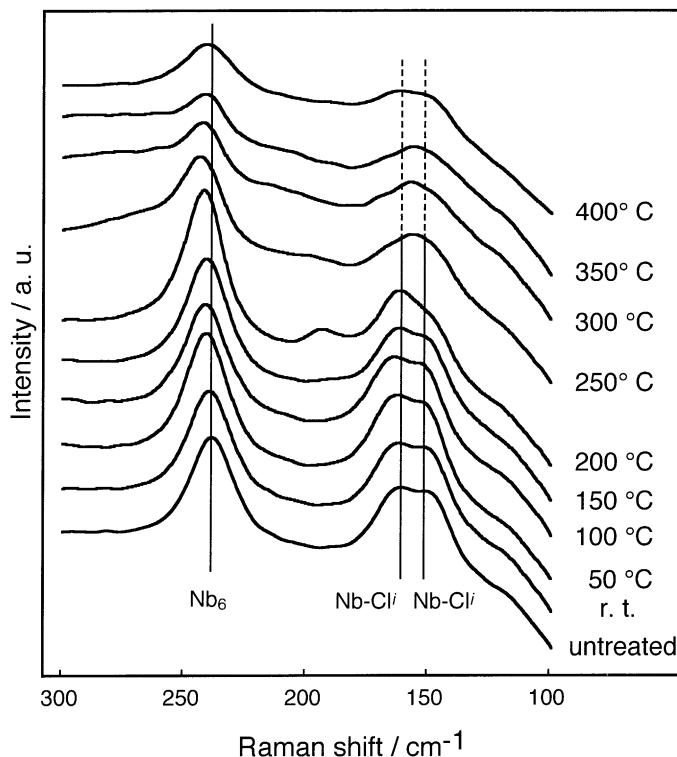
Fig. 5. Raman spectra of $[(Nb_6Cl_{12})Cl_2(H_2O)_4]\cdot 4H_2O$ (**1**) treated with H_2 (40 ml/min) for 1 h.

are shown in Fig. 5. The spectra markedly changed beyond 200 °C with increasing temperature. The Raman shift caused by the vibration of Nb–Cl^a or Nb–O has not been attributed for complex **1**. However, the peak at 239 cm^{-1} is assigned to the breathing motion of the Nb$_6$ octahedron (A$_{1g}$), whereas those at 161 and 152 cm^{-1} are attributed to edge bridging Nb–Cl^i breathing vibrations (E$_g$ and T$_{2g}$, respectively) [33]. Crystal structure data revealed that the differences in M–M distances parallel the observed variations in the Raman shift. The variations of the observed shift of the M$_6$ A$_{1g}$ band are almost entirely accounted for by differences in the M–M force constant that accompany differences in the M–M bond distances, and not by differences in mixing of the M–M and M–X^i or M–X^a coordinates [34]. The peak attributed to the Nb$_6$ A$_{1g}$ vibration mode begins to shift to higher energy by treatment at 150 °C and had the greatest shift at 250 °C. The loss of some internal Cl ligands can increase the Nb–Nb bond order of the Nb$_6$ octahe-

dron, which may be ascribed to the higher energy shift. However, the Nb$_6$ metal framework remained the same up to 400 °C. Above 200 °C, the two Raman peaks originally at 161 and 152 cm^{-1} due to edge bridging Nb–Cl^i breathing vibrations, were replaced with a new peak at the middle position, suggesting that the structure of the coordinating Cl ligands changed above this temperature. It is at this temperature that the catalytic activity emerged. No appreciable changes of these Raman spectra have been observed after 5 h reactions with 1-hexene at the same temperature. The formation of coke possibly suppressed this reaction.

Evolution of HCl gas was detected when **1** was treated above 150 °C, and a violent evolution began when treated above 200 °C. The evolution of Cl$_2$ gas was not however detected up to 500 °C. The $[(Nb_6Cl_{12})Cl_2(H_2O)_4]$ moiety of **1** is neutral and even if it converts to the corresponding extended solid state complex Nb$_6$Cl$_{14}$ ($[Nb_6Cl^i_{10}Cl^{i-a}_{2/2}]$ $Cl^{a-i}_{2/2}Cl^{a-a}_{4/2}$) [35], no evolution of HCl occurs, as shown in Eq. (1)

Scheme 1.

and Scheme 1.

$[(Nb_6Cl_{12})Cl_2(H_2O)_4] \cdot 4H_2O$ (**1**)
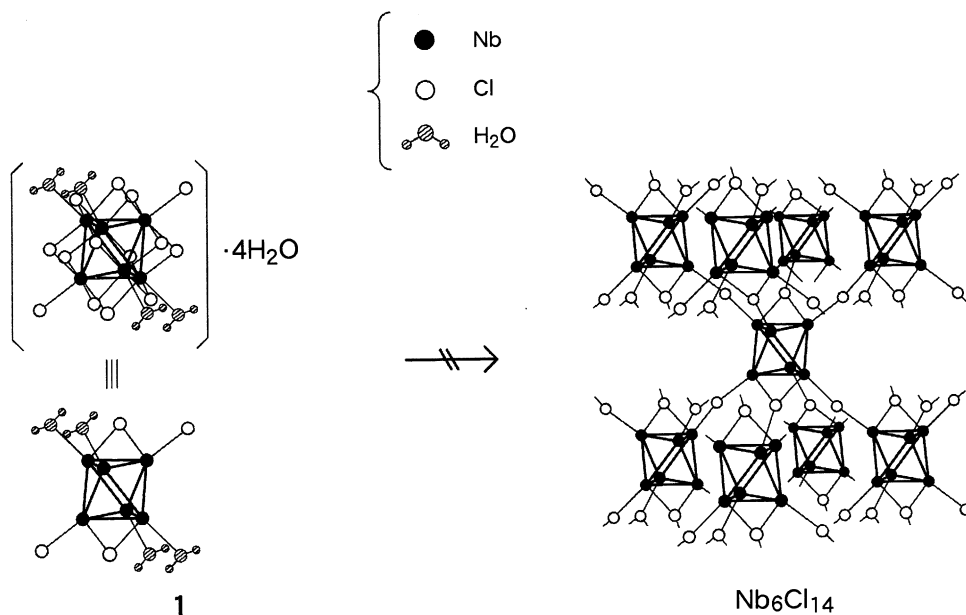
$\twoheadrightarrow Nb_6Cl_{14} + 8H_2O$ (1)
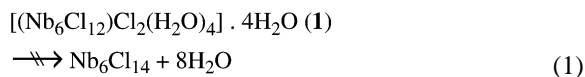
However, HCl could be produced by disproportiona-tion of **1**, as exemplified by Eqs. (2)–(4) to form Nb–O species. In this case, hydrogen operated not chemically

but physically to remove the produced HCl, which accords with the observation that the reactivity of **1** treated in a stream of helium exhibited almost the same reactivity, as presented in Table 1.
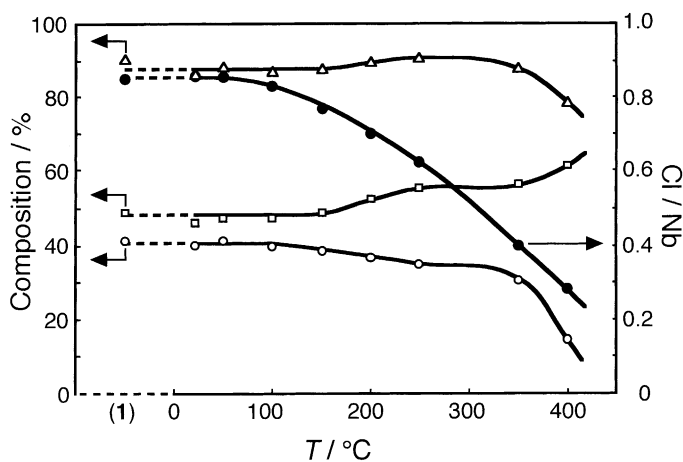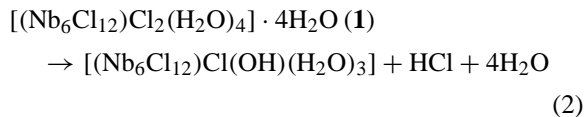
$[(Nb_6Cl_{12})Cl_2(H_2O)_4] \cdot 4H_2O$ (**1**)

$\rightarrow [(Nb_6Cl_{12})Cl(OH)(H_2O)_3] + HCl + 4H_2O$

(2)

Fig. 6. Analytical data of the treated sample of $[(Nb_6Cl_{12})Cl_2(H_2O)_4] \cdot 4H_2O$ (**1**) with H_2 (40 ml/min) for 1 h. Analytical data of intact **1** are also plotted. Nb ($\square$), Cl ($\bigcirc$), rest of Nb and Cl ($\triangle$), and relative ratio of Cl/Nb ($\bullet$).
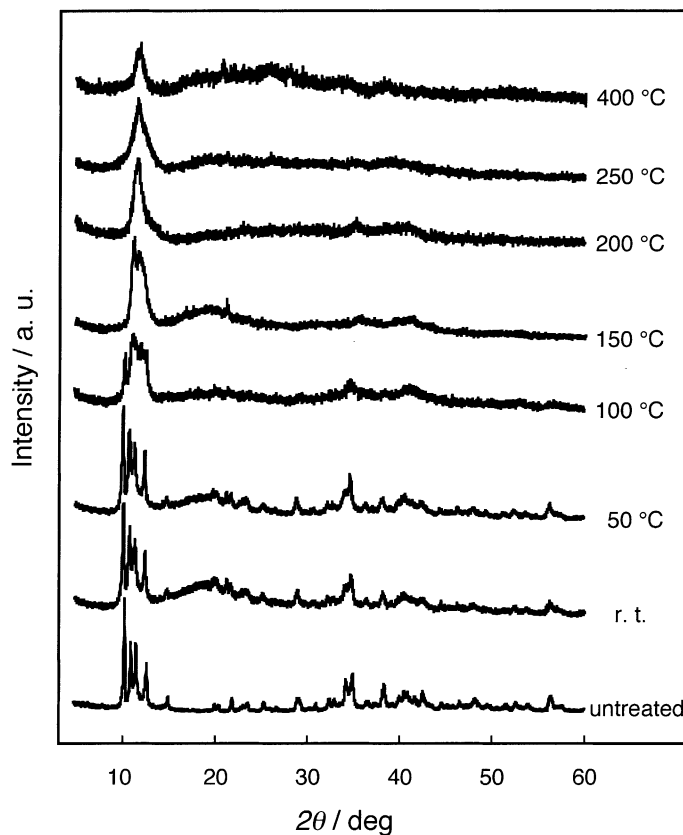
Fig. 7. XRD pattern of $[(Nb_6Cl_{12})Cl_2(H_2O)_4]\cdot 4H_2O$ (**1**) treated with H_2 (40 ml/min) for 1 h.
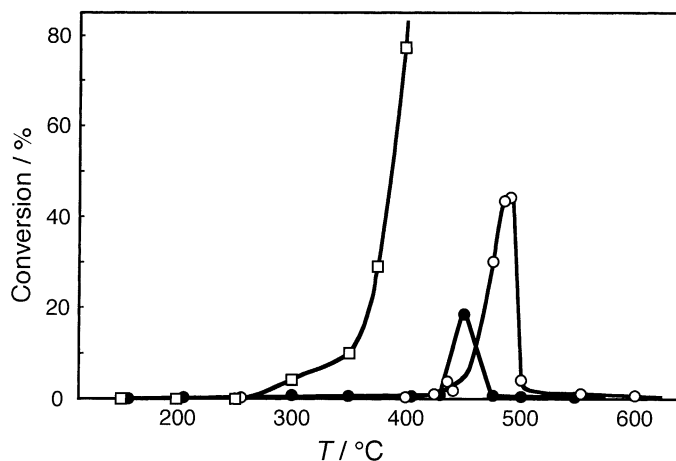
Fig. 8. Effect of treatment temperature on catalytic activity of $(H_3O)_2[(W_6Cl_8)Cl_6]\cdot 6H_2O$ (**2**). After treatment of **2** at various temperatures for 1 h with H_2, reactions proceeded at the same temperature (□). After treatment of **2** at various temperatures for 1 h with H_2, reactions proceeded at 150 °C (●) and 250 °C (○). Other conditions are the same as in Fig. 3. Conversion = (2-hexene + hexane)/(1-hexene + 2-hexene + hexane) × 100 (%) at 4 h after the reaction started.

$[(Nb_6Cl_{12})Cl(OH)(H_2O)_3]$

$$\rightarrow [(Nb_6Cl_{12})(OH)_2(H_2O)_2] + HCl \qquad (3)$$

$[(Nb_6Cl_{12})Cl(OH)(H_2O)_3]$

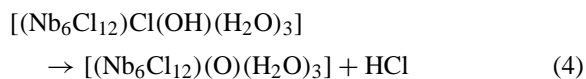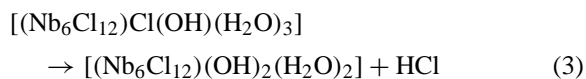$$\rightarrow [(Nb_6Cl_{12})(O)(H_2O)_3] + HCl \qquad (4)$$

Fig. 6 shows analytical data of Cl and Nb atoms in the treated samples. The Cl content of **1** started

decreasing when treated above 150 °C. Fig. 6 also shows that the relative amount of Cl to Nb, which is not volatile unless changed to $NbCl_x$ ($x = 2$, 3 or 5) or $NbClO_3$, decreased with an increase in the treatment temperature, and that experimentally, $Nb_6Cl_{11.0}$ species on average were formed by the treatment at 200 °C. The total amounts of Nb and Cl of the treated samples are around 90%, as Fig. 6 shows, and
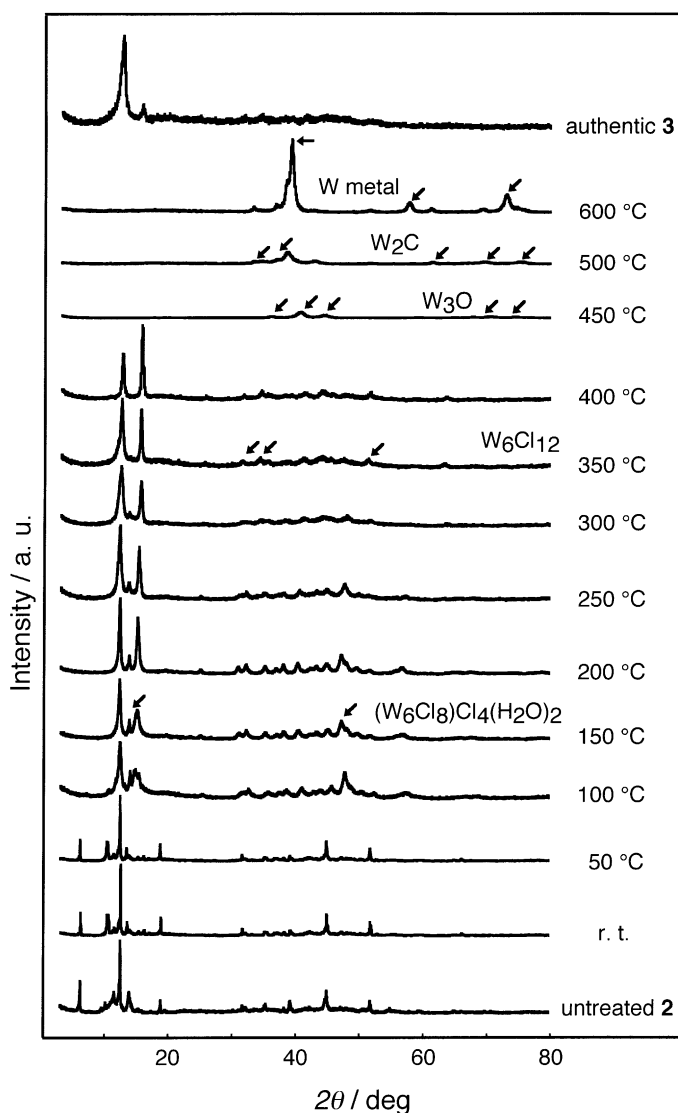

Fig. 9. XRD pattern of $(H_3O)_2[(W_6Cl_8)Cl_6]\cdot 6H_2O$ (**2**) treated with H_2 (40 ml/min) for 1 h. The XRD pattern of authentic W_6Cl_{12} (**3**) is also shown. Both of the identified compounds, $[(W_6Cl_8)Cl_4(H_2O)_2]$ and **3**, have two strong diffraction peaks at 12.4–12.6 and 15.3–15.6°; hence, unique diffraction peaks of each compound are indicated.

therefore some components presumably originating from the water contained in **1** were left in the treated cluster samples. Assuming that the rest is composed of oxygen or the hydroxyl group, the experimental formula of the 200 °C-treated sample is $Nb_6Cl_6O_{7.2}$ or $Nb_6Cl_6(OH)_{6.8}$. Hence, the catalytic activity of the cluster can be attributed to the acid site of the Nb–O moiety or the surface hydroxyl group with retention of the octahedral metal framework.

The X-ray diffraction patterns of **1** treated in the same way are shown in Fig. 7. The change of the X-ray diffraction pattern reveals that treatment above 100 °C changes **1** to an amorphous compound that is not the extended solid state compound Nb_6Cl_{14} prepared by another route. Furthermore, the change of the crystal structure did not give rise to the catalytic activity.

3.3. Catalysis by $(H_3O)_2[(W_6Cl_8)Cl_6]\cdot 6H_2O$ (**2**)

Fig. 8 presents the catalytic activities of W cluster **2** after preliminary treatment at varying temperatures for 1 h, followed by the reaction at the same temperature. The activity commenced when the preliminary treatment and the following reaction were carried out at 300 °C, and the activity markedly increased with increasing temperature. On the other hand, while the

samples treated at various temperatures react at 150 and 250 °C, the maximum activities appeared around 450 and 480 °C, respectively. The X-ray diffraction patterns of **2** treated at various temperatures in hydrogen streams for 1 h are presented in Fig. 9, with the pattern of W_6Cl_{12} ($[W_6Cl_8^i]Cl_2^aCl_{4/2}^{a-a}$) (**3**) synthesized independently. Fig. 9 shows that the cluster changed at above 100 °C from $(H_3O)_2[(W_6Cl_8)Cl_6]\cdot 6H_2O$ (**2**) via $[(W_6Cl_8)Cl_4(H_2O)_2]$ [36,37] to an extended W–Cl–W bonded solid state compound **3** [38] as heat was applied up to 400 °C (Scheme 2). The complex decayed to an amorphous compound by 450 °C, while very weak broad peaks attributable to W_3O and W_2C were observed at 450 and 500 °C, respectively. Finally, it was reduced to metallic W at 600 °C. The temperature (300 °C) at which the catalytic activity commenced is the decomposition temperature of $[(W_6Cl_8)Cl_4(H_2O)_2]$, as shown in Fig. 8. The temperatures (450−480 °C) at which the maximum activity is observed is the decomposition temperature of **3**. In both cases, degradation of the crystal structures relates to the catalytic activity.

The Raman spectra of **2** treated at various temperatures in hydrogen streams for 1 h are illustrated in Fig. 10, with the spectrum of **3** synthesized independently. Characterizations of the peaks of $[(W_6Cl_8)$-
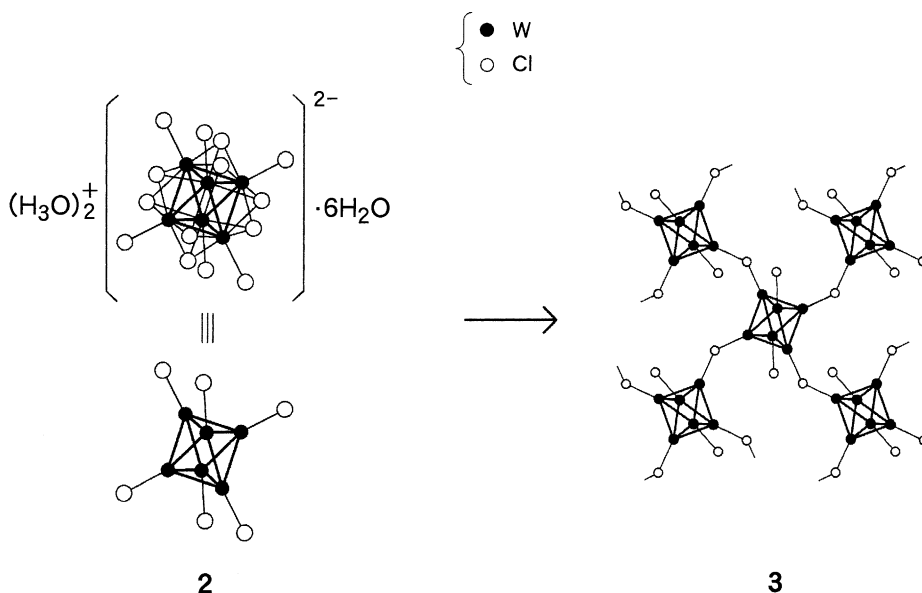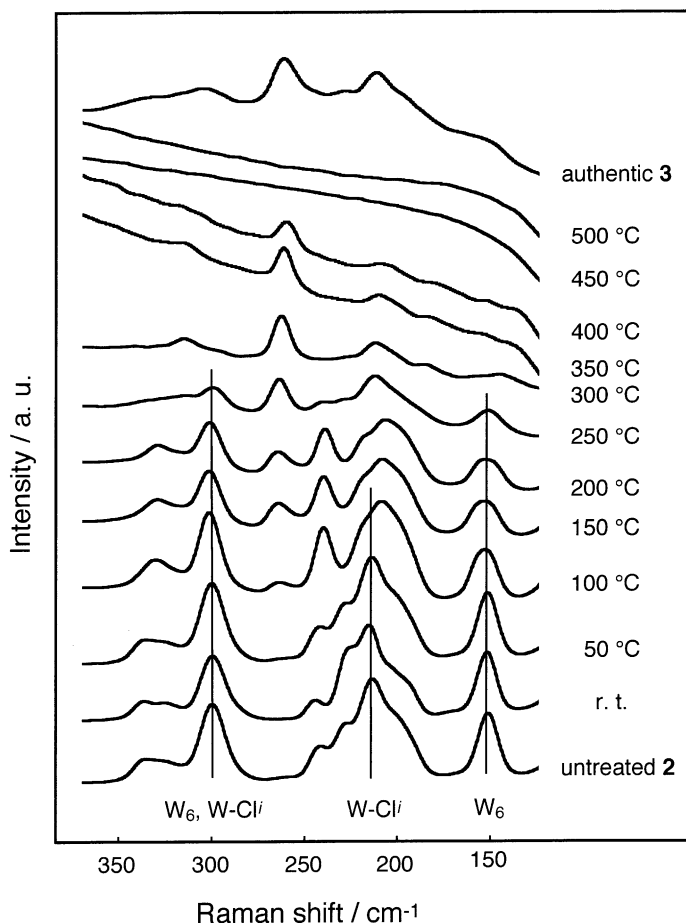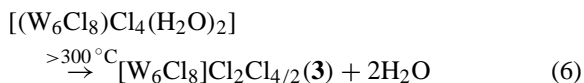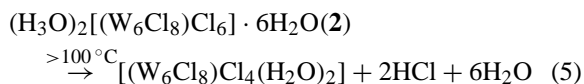

Scheme 2.

Fig. 10. Raman spectra of $(H_3O)_2[(W_6Cl_8)Cl_6]\cdot 6H_2O$ (**2**) treated at various temperatures with H_2 (40 ml/min) for 1 h. The Raman spectrum of authentic W_6Cl_{12} (**3**) is also shown.

$Cl_4(H_2O)_2]$ and **3** are not available, although that of **2** has been reported [34]. The peak due to the breathing motion of the W_6 octahedron A_{1g} accidentally overlaps that of the W–Cl^i cage breathing mode at $300 \, cm^{-1}$. This peak and the assigned peak of the W–W vibration of W_6 at $153 \, cm^{-1}$ of cluster **2** almost disappeared at 300 °C, and then the catalytic activity developed. The spectra of 300, 350 and 400 °C-treated samples are almost the same as that of the authentic sample of cluster **3**. At 450 °C, most of the Raman peaks disappeared, and the maximum catalytic activity appeared. These findings suggest that the structural change from **2** to **3** brought about the catalytic activity, and th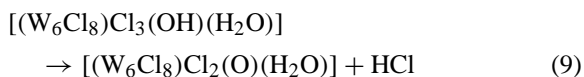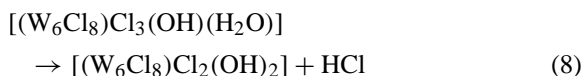at decomposition of the molecular structure of **3** brought about the maximum catalytic activity. This would be in accord with the results of X-ray analyses. No appreciable changes of the Raman spectra or the XRD patterns were observed after subsequent 5 h reactions with 1-hexene at the same temperatures.

Intense evolution of HCl was confirmed by preliminary treatment above 100 °C, although Cl_2 was not detected during this time. The evolution of HCl, however, does not necessarily demonstrate the formation of the Cl-deficient cluster species, since the $[(W_6Cl_8)Cl_6]$ moiety of **2** is a dianion bearing two protons, and the change of **2** to the complex $[(W_6Cl_8)Cl_4(H_2O)_2]$ accompanies the evolution of HCl, as described in

Eq. (5). The next step in the conversion to **3** does not release HCl, as shown in Eq. (6).

$$(H_3O)_2[(W_6Cl_8)Cl_6] \cdot 6H_2O \mathbf{(2)}$$
$$\overset{>100\,°C}{\rightarrow} [(W_6Cl_8)Cl_4(H_2O)_2] + 2HCl + 6H_2O \quad (5)$$

$$[(W_6Cl_8)Cl_4(H_2O)_2]$$
$$\overset{>300\,°C}{\rightarrow} [W_6Cl_8]Cl_2Cl_{4/2} \mathbf{(3)} + 2H_2O \quad (6)$$

Nevertheless, the evolution of HCl was detected above $300\,°C$, which indicates that the same reaction as in the case of the Nb cluster took place as exemplified in Eqs. (7)–(9).

$$[(W_6Cl_8)Cl_4(H_2O)_2]$$
$$\rightarrow [(W_6Cl_8)Cl_3(OH)(H_2O)] + HCl \quad (7)$$

$$[(W_6Cl_8)Cl_3(OH)(H_2O)]$$
$$\rightarrow [(W_6Cl_8)Cl_2(OH)_2] + HCl \quad (8)$$

$$[(W_6Cl_8)Cl_3(OH)(H_2O)]$$
$$\rightarrow [(W_6Cl_8)Cl_2(O)(H_2O)] + HCl \quad (9)$$
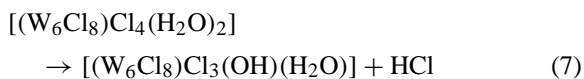
Chemical analysis of the $400\,°C$-treated sample revealed that the W content was 72.41% and the Cl content was 26.65%, and accordingly, the rest amounts to 0.94%. The experimental error inherent in each analysis is estimated to be $\pm0.5\%$, and hence total error is $\pm0.71\%$. The formation of W_3O as a minor component in the $450\,°C$-treated sample, as Fig. 9 shows, also supports some oxygen atoms being retained in the treated samples. Thus, a small amount of oxygen moiety may be left in this $400\,°C$-treated sample, and the empirical formula is $W_6Cl_{11.5}(O)_{0.9}$ or $W_6Cl_{11.5}O(OH)_{0.8}$.

The authentic sample of **3** exhibited an X-ray diffraction pattern and Raman spectrum as shown in Figs. 9 and 10: both the pattern and the spectrum are practically in accord with those of the sample treated at $300-400\,°C$, suggesting the formation of stable solid state **3** by the treatment. This conflict may be interpreted in terms of the formation of an imperfect crystal containing a defective $[W_6Cl_8^i]Cl_2^aCl_{4/2}^{a-a}$ moiety exhibiting catalytic activity. In other words, small amounts of the foreign cluster, which has the catalytic activity, were held in the crystal lattice of $\{[W_6Cl_8^i]Cl_2^aCl_{4/2}^{a-a}\}_n$ up to ca. $450\,°C$. In contrast, the defective moiety $[Nb_6Cl_{12}]$ in **1**, which has maximum

activity by preliminary treatment around $200\,°C$, was not retained as a solid state cluster. Hence, the activity waned at treatment temperatures as low as $250\,°C$. The catalytically active species were probably oxo or hydroxo clusters with acidic character.

4. Conclusion

Molecular halide clusters of Nb, Mo, Ta and W are stable complexes showing no catalytic activity. However, preliminary treatment at $250\,°C$ gave them catalytic activity for double bond isomerization of the olefin. When the Nb cluster **1** was treated in a hydrogen stream with increasing temperatures, the crystal structure was found to decay above $100\,°C$. However, the molecular structure changed around $200\,°C$ by losing some of the Cl ligands, leaving the Nb_6 cluster metal framework intact. The temperature at which the catalytic activities appeared was in accord with that of the change of the molecular structure. In the case of W cluster **2**, the catalytic activity appeared on treatment at $300\,°C$, at which temperature the discrete molecular cluster $[(W_6Cl_8)Cl_4(H_2O)_2]$ changed to the solid state cluster **3**. The catalytic activity was enhanced with increasing temperature up to the decay of **3** at around $450\,°C$. Retention of the catalytic activity at higher temperatures can be attributed to retention of the catalytically active defective moiety in the network of the solid state cluster **3**. In both clusters, the active species would be oxo or hydroxo clusters of solid acid character.

References

[1] S.C. Lee, R.H. Holm, Angew. Chem., Int. Ed. Engl. 29 (1990) 840.
[2] F.A. Cotton, T. Hughbanks, C.E. Runyan Jr., W.A. Wojtczak, in: M.H. Chisholm (Ed.), Early Transition Metal Clusters with π-Donor Ligands, VCH Publishers, New York, 1995, Chapter 1, p. 1.
[3] T. Saito, in: M.H. Chisholm (Ed.), Early Transition Metal Clusters with π-Donor Ligands, VCH Publishers, New York, 1995, Chapter 3, p. 63.
[4] A.W. Struss, J.D. Corbett, Inorg. Chem. 17 (1978) 965.
[5] H. Imoto, J.D. Corbett, A. Cisar, Inorg. Chem. 20 (1981) 145.
[6] T. Chihara, S. Kamiguchi, Chem. Lett. (2002) 70.
[7] N. Prokopuk, D.F. Shriver, Adv. Inorg. Chem. 46 (1999) 1.
[8] I. Nowak, M. Ziolek, Chem. Rev. 99 (1999) 3603.
[9] G.J. Miller, J. Alloys Compd. 229 (1995) 93.

[10] T. Chihara, H. Yamazaki, J. Organomet. Chem. 473 (1994) 273.
[11] S. Siegel, J. Catal. 30 (1973) 139.
[12] M. Hudlichy, Reduction in Organic Chemistry, Ellis Horwood, West Sussex, 1984.
[13] P. Rylander, Catalytic Hydrogenation in Organic Synthesis, Academic Press, New York, 1979.
[14] M. Freifelder, Catalytic Hydrogenation in Organic Synthesis, Procedures and Commentary, Wiley, New York, 1978.
[15] M. Freifelder, Practical Catalytic Hydrogenation, Wiley, New York, 1971.
[16] F.H.C. Edgecombe, Tetraherdon Lett. 24 (1962) 1161.
[17] F.W. Koknat, J.A. Parsons, A. Vongvusharintra, Inorg. Chem. 13 (1974) 1699.
[18] P. Nannelli, B.P. Block, Inorg. Synth. 12 (1970) 170.
[19] V. Kolesnichenko, L. Messerle, Inorg. Chem. 37 (1998) 3660.
[20] G.M. Ehrlich, P.E. Rauch, F.J. Disalvo, Inorg. Synth. 30 (1995) 1.
[21] H.S. Broadbent, G.C. Campbell, W.J. Bartley, J.H. Johnson, J. Org. Chem. 24 (1959) 1847.
[22] H.S. Broadbent, L.H. Slaugh, N.L. Jarvis, J. Am. Chem. Soc. 76 (1954) 1519.
[23] R. Maurel, M. Guisnet, L. Bove, Bull. Sco. Chim. Fr. (1969) 1975.
[24] J.E. Kilpatrick, E.J. Prosen, K.S. Pitzer, F.D. Rossini, J. Res. Natl. Bur. Stand. 36 (1946) 559.
[25] H. Hattori, Chem. Rev. 95 (1995) 537.
[26] M.J. Baird, J.H. Lunsford, J. Catal. 26 (1972) 440.
[27] T. Yamaguchi, H. Sasaki, K. Tanabe, Chem. Lett. (1973) 1017.
[28] Y. Imizu, T. Yamaguchi, H. Hattori, K. Tamabe, Bull. Chem. Soc. Jpn. 50 (1977) 1040.
[29] T. Iizuka, K. Ogasawara, K. Tanabe, Bull. Chem. Soc. Jpn. 56 (1983) 2927.
[30] H. Hattori, N. Asada, K. Tanabe, Bull. Chem. Soc. Jpn. 51 (1978) 1704.
[31] J. Abott, B.W. Wojciechowski, J. Catal. 90 (1984) 270.
[32] J. Abbot, A. Corma, B.W. Wojciechowski, J. Catal. 92 (1985) 398.
[33] K. Harder, W. Preetz, Z. Anorg. Allg. Chem. 591 (1990) 32.
[34] J.R. Schoonover, T.C. Zietlow, D.L. Clark, J.A. Heppert, M.H. Chisholm, H.B. Gray, A.P. Sattelberger, W.H. Woodruff, Inorg. Chem. 35 (1996) 6606.
[35] A. Simon, H.G. Schnering, H. Wöhrle, H. Schäfer, Z. Anorg. Allg. Chem. 339 (1965) 155.
[36] H. Schäfer, H. Plautz, Z. Anorg. Allg. Chem. 389 (1972) 57.
[37] L.J. Guggenberger, A.W. Sleight, Inorg. Chem. 8 (1969) 2041.
[38] R.E. McCarley, T.M. Brown, Inorg. Chem. 3 (1964) 1232.